A Comparative Study of Optimal Fuzzy Logic Controllers for Blade Pitch Angle in Horizontal-axis Wind Turbines

Adnan Qahtan Adnan*‡, Mohammed Khalil Hussain*

*Department of Energy Engineering, University of Baghdad, 10074, Baghdad, Iraq

(a.adnan1609@coeng.uobaghdad.edu.iq, mohammedkhalil@uobaghdad.edu.iq)

‡Corresponding Author

"‡Adnan Qahtan Adnan, 10074, Tel: + 964 7816793819, a.adnan1609@coeng.uobaghdad.edu.iq"

Received: 02.01.2024 Accepted:20.01.2024

Abstract- The blade pitch angle (BPA) in wind turbine (WT) is controlled to maximize output power generation above the rated wind speed (WS). In this paper, four types of controllers are suggested and compared for BPA controller in WT: PID controller (PIDC), type-1 fuzzy logic controller (T1-FLC), type-2 fuzzy logic controller (T2-FLC), and hybrid fuzzy-PID controller (FPIDC). The Mamdani and Sugeno fuzzy inference systems (FIS) have been compared to find the best inference system used in FLC. Genetic algorithm (GA) and Particle swarm optimization algorithm (PSO) are used to find the optimal tuning of the PID parameter.The results of 500-kw horizontal-axis wind turbine show that PIDC based on PSO can reduced 2.81% in summation error of power signal (EPS) than GA. T1-FLC based on Sugeno FIS performs 23.98% lower summation of EPS than T1-FLC based on Mamdani FIS and 27.63% lower than optimal PIDC when using PSO. Sugeno FIS in T2-FLC provides 21.81% lower summation of EPS than Mamdani FIS in T2-FLC and lower summation of EPS than T1-FLC based on Sugeno FIS. On the other hand, the hybrid type-2 fuzzy-PID controller (T2-FPIDC) based on PSO with the Sugeno FIS provides 21.93% lower summation of EPS than the Sugeno FIS in hybrid T2-FPIDC based on GA as well as 90% lower summation of EPS than Sugeno T2-FLC. Finally, the proposed optimal hybrid T2-FPIDC based on PSO and Sugeno FIS provides the best results in terms of consistent output power at fluctuating wind speeds and lowest in summation of EPS.

Keywords Wind Turbine, Type-2 fuzzy logic controller, fuzzy inference systems, hybrid fuzzy-PID controller, particle swarm optimization, genetic algorithm.

Nomenclature:

BPA	Blade Pitch Angle
Cp	Power Coefficient
EPS	Error of Power Signal
FIS	Fuzzy Inference System
GA	Genetic Algorithm
PAC	Pitch Angle Control
PIDC	Pid Controller
PSO	Particle Swarm Optimization
T1-FLC	Type-1 Fuzzy Logic Controller
T1-FPIDC	Type-1 Fuzzy-PID Controller
T2-FLC	Type-2 Fuzzy Logic Controller
T2-FPIDC	Type-2 Fuzzy-PID Controller
TSR	Tip Speed Ratio
WS	Wind Speed
WT	Wind Turbine

Romans:

P_{ac}	Actual Power Outputs	[w]
k_d	Derivative Gain	-
k_i	Integral Gain	-
P_{el}	Electrical Power	[w]
P_m	Mechanical Power	[w]
k_p	Proportional Gain	-
P_{ref}	Reference Power Outputs	[w]
T_m	Turbine Mechanical Torque	[N.m]
W_{ac}	Actual Wind Speed	[m/s]
v	Wind Speed	[m/s]
C_p	Power Coefficient	-

1. Introduction

Today's need for renewable energy is due to a variety of issues affecting the world, including environmental degradation and global warming. Since the end of the 1970s, WT has grown quickly as the main source of renewable energy. WT can generate electric energy from wind energy without any environmental hazards [1, 2]. Both horizontal and vertical axis WT are used to generate the electricity. However, it has been found that horizontal-axis wind turbines extract more power than vertical-axis wind turbines [3].

The BPA in WT plays a significant role to regulate the power generation of WT [4]. Also, it helps to minimize the fatigue load exerted on the turbine's related components. When the WS exceeds the rated speed, pitch angle control (PAC) is used to keep the output power at the rated power [5]. In medium to large-scale WT, Pitch angle control is used in order to maintain the power generation close to the rated value by using either PID controllers (PIDC) or artificial intelligence controllers [6].

Pitch angle control system by using PIDC is frequently used to maintain the captured wind energy close to the rated value [7, 8].When the WS exceeds the turbine's rated speed, a PIDC is designed to manage the BPA of WT. PID controller has been applied to improve the performance BPA controller of WT when the PID parameters (kp, ki, and kd) are selected based on the root locus method or neural network algorithm [9]. On the other hand, in advanced design approaches, modeling, simulation, and computational optimization are necessary. Particle Swarm Optimization (PSO) and the Genetic Algorithm (GA) are the most widely used techniques for optimizing nonlinear and highly complicated problems [10]. A multi-objective particle swarm optimization (PSO), and Genetic algorithm (GA) are compared to find the optimal tunning of PID parameters and the results shows PID controller based PSO has better output power flow and the dynamic response than PID controller-based GA [11, 12].

Fuzzy logic controller (FLC) is now the most often used for controlling nonlinear systems [13]. When obtaining an accurate mathematical representation of the system poses a challenge, FLC is becoming more popular due to it is ability to use expert knowledge in the control design as well as it can improve the flexibility of nonlinear systems in the presence of fluctuations or uncertainty [14-16].T1-FLC based on Mamdani FIS is applied and showed a suitable controller for BPA in WT [17-20]. Also, T1-FLC based on Sugeno FIS is controlled WT in actual WS [21]. On the other hand, the effectiveness of the T2-FLC has been evaluated for BPA controller and showed that the T2-FLC gives higher enhancement in power quality and transient stability than T1-FLC [22-26].

The hybrid fuzzy-PID controllers is a combination of fuzzy logic controllers with PIDC. The hybrid type-1 fuzzy PID controller performed better BPA controller of WT than PIDC and T1-FLC in [27,28], Optimal hybrid T1-FPIDC based on GA has been applied and achieving improvements in output power and structure stability of Floating offshore wind turbines [29,30].

Considering the state of the art for BPA controllers to get stable output power, this paper compares different controllers and proposes a novel AIC for BPA controller in WT. A 500-kw HAWT at actual WS is presented to calculate the output power and show the effect of BPA in WT. Four controllers have been evaluated and compared: optimal PIDC, T1-FLC, T2-FLC, and optimal hybrid T2-FPIDC. The first contribution of this paper compares two FIS (Mamdani and Sugeno) in design T1-FLC and T2-FLC. Another contribution of this paper is to propose the optimal hybrid T2-FPIDC by using GA and PSO algorithms to find the best BPA controller. The results demonstrate that the optimal hybrid T2-FPIDC based on the Sugeno FIS and PSO algorithm can provide the best results in terms of stable output power at variable WS.

2. Characteristics of Wind Turbine

The main purpose of WT is to produce electrical power from the WS. The characteristic of power performance in WT is called power curve and it represents the relation between the output power and WS. Therefore, the turbine speed needs to be controlled while WT is in operation. In both high and low WS scenarios, this control technique aims to safeguard turbine systems and enhance the output power. The output power of the WT has four operation zones depending on varying WS and BPA, as shown in Figure 1. When the cut-in speed in the zone (I.) is greater than the WS, the output power is zero. The zone (II.), which is halfway between the cut-in speed and the rated speed, has the highest power point tracking. Between the cut-out speed and the rated speed is the zone (III). Finally, WT is stopped in the zone (IV.) because WS has exceeded the cut-out speed [21].

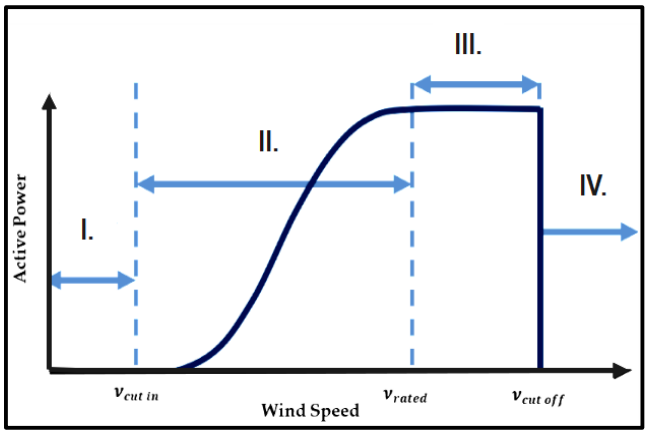

Fig. 1. Characteristic curve of the wind turbine.

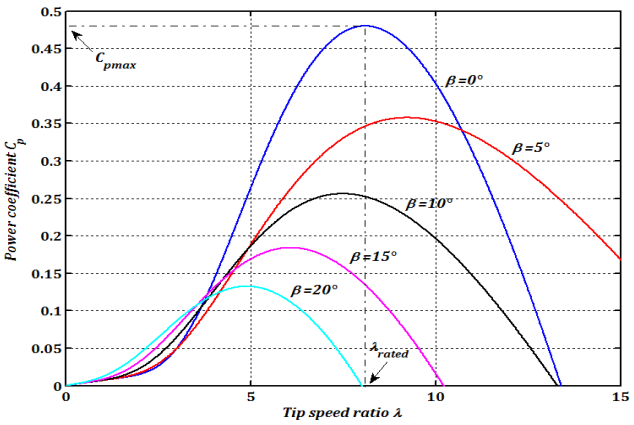

Fig. 2. Power coefficient in different pitch angle.

One of the key variables in determining the power generation of WT is the power coefficient (Cp). Cp is changed by the tip speed ratio (λ) and pitch angle (β). As shown in Figure 2, Cp describes how effectively WT produces power. The turbine speed is calculated using Cp and tip speed ratio (TSR). Furthermore, based on various values of pitch angle, TSR and Cp are changed. Figure 2 demonstrates that Cp is in maximum when the β is zero. When WS is changed, the TSR is changed too. Therefore, WT can operate at the most effective level at a specific WS [21].

3. Wind Turbine Mathematical Model

The mathematical model of WT is explained in this part after considering the effect of BPA in operation of WT. The power generation of WT can be calculated by using the formula below.

$$P_w = 0.5\,\rho\,A\,v^3 \quad (1)$$

Where (P_w) is the wind power (Watt), (ρ) is the air density (kg /m^3), (A) is the blades swept area (m^2), and (v) is WS (m/s). The mechanical power generation of WT can be calculated as below.

$$P_m = P_w\,C_p\,(\beta, \lambda) \quad (2)$$

The mechanical power (P_m) of WT is calculated by using equations (1) and (2).

$$P_m = 0.5\,\rho\,A\,v^3\,C_p\,(\beta, \lambda) \quad (3)$$

Since Cp is extremely nonlinear, it changes depending on β and TSR, as illustrated below.

$$C_p = 0.5\left(\frac{116}{\lambda_i} - 0.4\,\beta - 5\right)e^{\left(-\frac{21}{\lambda_i}\right)} + 0.0068\,\lambda \quad (4)$$

The Cp value is produced by swapping the (λi) value in (5) with the one in (4). Here, using the value of the intermediate variable (λi), which is represented by the following equation:

$$1/\lambda i = 1/(\lambda + 0.08\,\beta) - 0.035/(3\,\beta + 1) \quad (5)$$

Tip speed ratio (λ) is the mechanical angular speed of the blades that related with WS, and it is expressed as follows:

$$\lambda = (w_{wt} * R)/(v) \quad (6)$$

where (w_{wt}) is the rotor's angular speed and (R) is the WT blade radius. Any change in rotor speed or WS has an impact on the Cp, which is affected by the TSR. As a result, the output power is changed. The mechanical torque and electrical power are given below.

$$P_{el} = 0.5\,\rho\,A\,v^3\,C_p\,(\beta, \lambda)\,\eta_{gen} \quad (7)$$

$$T_m = P_{el} * w_{wt} \quad (8)$$

Where (P_{el}) is the electrical power of WT, (η_{gen}) is the generator efficiency, and (T_m) is mechanical torque of WT.

4. Blade Pitch Angle Controllers Design

This section illustrates four different control methods for the BPA controller: PIDC, T1-FLC, T2-FLC, and hybrid T2-FPIDC. These controller techniques are used to keep the power generation of WT at a stable region.

4.1. PIDC Design

PIDC produces the output signals based on the controlled objective [11]. PIDC has three controller gains (k_p , k_i, and k_d) that selected to find the lowest error signals to WT as shown in Figure. 3.

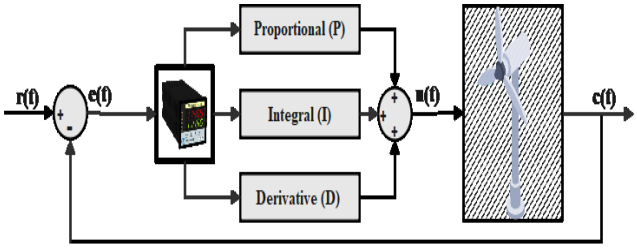

Fig. 3. PID controller structure for wind turbine.

Where u(t) is output of control, c(t) is the output of WT controlling system, r(t) is the reference input, and e(t) is error.

4.2. FLC Design

This section presents the operating principles for two types of FLC applied in WT: T1-FLC and T2-FLC with two FIS (Mamdani and Sugeno). In general, FLC involves fuzzification, defuzzification, fuzzy inference systems, and the rule base. Each object in FLC is assigned a membership function (MF) degree between [0, 1] [31].

T1-FLC is stated with a degree of truth that is represented as a number in the interval [0, 1]. Figure. 4 shows the main parts of T1-FLC. The quantized input data are converted into suitable linguistic variables by using the fuzzifier. The inference is the main part of the FLC, it is specified the process that transforms fuzzy inputs into a fuzzy output after considering the fuzzy rules. In this paper, the Mamdani and Sugeno FIS are used and compared. Finally, defuzzification is producing the nonfuzzy (crisp) control actions based on the best represents of fuzzy control actions [31].

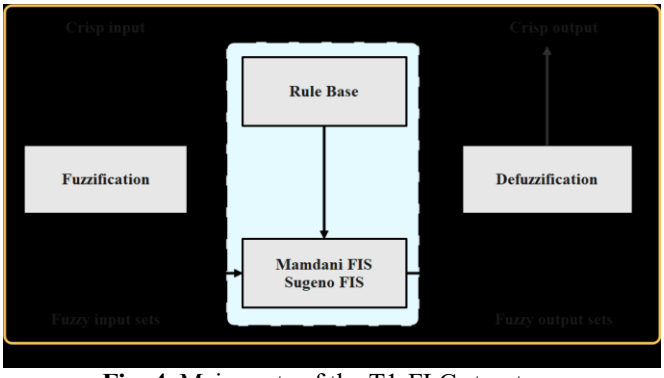

Fig. 4. Main parts of the T1-FLC structure.

As an extension of T1- FLC, T2- FLC is used to represent and address issues with a higher level of ambiguity and uncertain in MF [32]. Each MF is represented by an additional MF known as the secondary MF and it has been proposed to address the T1- FLC limitations when uncertainty is too high. Higher levels of uncertainty cannot be managed by T1- FLC because it can only assign a single-valued membership degree at each point in the universe of discourse. Consequently, T2-

FLC is applied another membership degree to the primary membership values. Therefore, it has the footprint of uncertainty and the type of reduction which makes it different from T1-FLC as shown in Figure. 5.

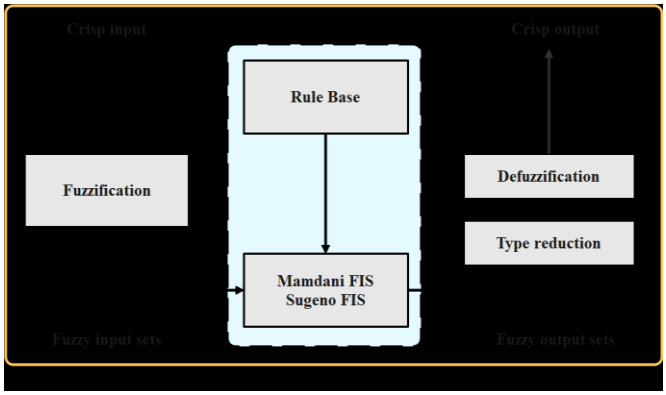

Fig. 5. Main parts of the T2-FLC structure.

4.3. Hybrid FPIDC Design

The hybrid fuzzy-PID controllers (H-FPIDCs) are a combination of fuzzy logic controllers with PIDC. In this paper, a design process for the fuzzy-PID controller is used to improve the BPA control system of WT. The hybrid system of control using a fuzzy-PID controller is illustrated in Figure 6 [33].

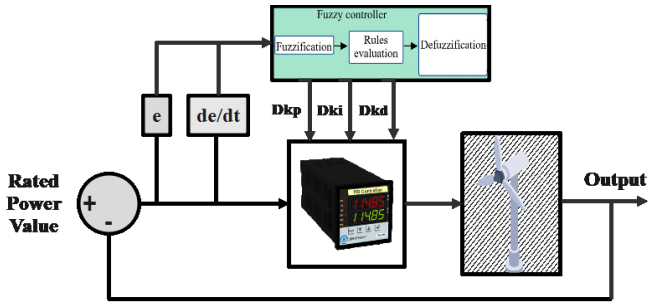

Fig. 6. Hybrid T2-FPIDC structure for WT.

5. Optimization Techniques for Optimal Controller

To obtain the optimal tuning of PID parameter values (kp, ki, and kd), in this paper PSO and GA are applied and compared to determine the optimal PID parameter for BPA controller. The five essential components in optimal PID parameter tuning are defined below.

5.1. Design Variables:

The main parameters of PIDC (kp, ki, kd) are defined as the design variables of the BPA controller in WT.

5.2. Objective Function:

minimized (min) the error signal in the power generation and WS is the main objective function. The total error (E) is calculated based on the summation of the absolute errors obtained from power (P) and speed (W).

$$min\, E = \sum \left| \left(P_{ac} - P_{ref} \right) + \left(W_{ac} - W_{ref} \right) \right| \qquad (9)$$

Where (P_{ac}) and (P_{ref}) are actual and reference power outputs, while (W_{ac}) and (W_{ref}) are actual and reference WS.

5.3. Constraints:

The Constraints of the PIDC are defined based on the minimum and maximum levels of each parameter as given below.

$$\begin{pmatrix} \underline{K_{pmin}} \le K_p \le \overline{K_{Pmax}} \\ \underline{K_{imin}} \le K_i \le \overline{K_{imax}} \\ \underline{K_{dmin}} \le K_d \le \overline{K_{dmax}} \end{pmatrix} \qquad (10)$$

where K_p , K_i, and K_d are the PID parameters; $\underline{K_{Pmin}}$, $\underline{K_{imin}}$, and $\underline{K_{dmin}}$ are the minimum levels of PID parameters; $\overline{K_{Pmax}}$, $\overline{K_{imax}}$ and $\overline{K_{dmax}}$ are the maximum levels of PID parameters.

5.4. Optimization Algorithms:

Genetic Algorithm and Particle swarm optimization are used to determine the best and optimal PID parameters as follow:

A. Genetic Algorithm (GA)

The evolutionary algorithm based on a biological process used to optimize complex objective functions is called GA. GA uses seven steps to determine the best design variables: parameter selection, decoding, and encoding, population size, natural selection, combining, mating, and mutations. GA repeats the steps until the GA is converged [34].

B. Particle Swarm Optimization (PSO)

A population of interacting elements that can find the optimal design variables through the space of search is defined as PSO. Experience is defined as interacting elements (particles) traveling (flying) in quest of space to locate the optimum position. In the search space, each interacting piece saves the optimal location and neighbourhood. PSO has seven steps to calculate the optimal design variables: defining the selection, finding the location, specifying the velocity vectors in each interacting element, finding the fitness values, calculating the locations, calculating the speed, and adjusting the location until the specified requirements are met [34,35].

5.5. Optimization Procedure:

This section shows the procedure to calculate the optimal PID parameter of BPA controller in WT. First step is defining the main component of the optimization algorithm: design variables, objective function, and constraints, and applying optimization algorithm (GA or PSO) as explained in previous section. Second step is computing output power, pitch angle, and wind speed based on initial PID parameters for actual WS. third step is calculating the objective function (min (E)) based on equation 9. Final step is finding the optimal value of (kp, ki, kd) after several iterations. Figure. 7 shows the flowchart of the optimization procedure to find the optimal PIDC parameter for the BPA controller of WT.

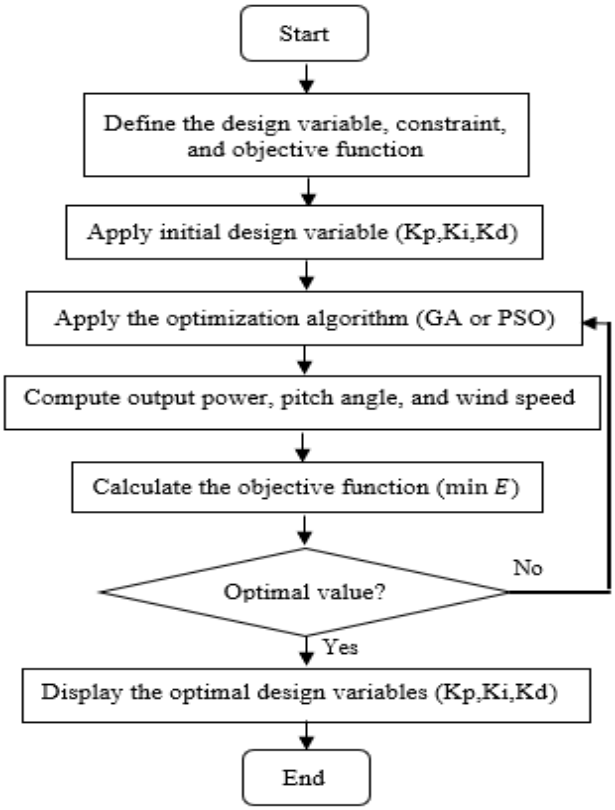

Fig. 7. Flowchart for the PIDC optimization process.

6. Simulation Results and Discussion

The simulation model and results of 500-kW HAWT are presented in this section. WT system has been tested for four different controllers based on actual WS data as shown in Figure. 8.

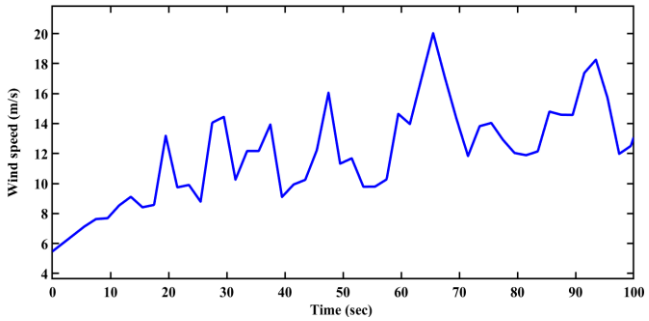

Fig. 8. WS of the 500-kw HAWT for 100s.

Table 1. provides a list of the specifications used to create the 500-kW HAWT model. The number of rotor blades on WT determines the ideal TSR. In this paper, TSR is considered (4.19). If the airfoil is carefully built, the optimal TSR could be approximately 25% to 30% higher than this ideal value. The ideal TSR may exceed the stated limits depending on the type of profile utilized [36]. Two MATLAB functions are utilized in the Simulink model for relevant operations in MATLAB simulation. The first function indicates the cut-in, while the second function indicates the cut-out. One is used to start the controller when it is operating at the nominal WS, while the other is used to stop the controller when it is operating above the nominal WS. Finally, Figure. 9 shows the entire WT system model, including different controllers. The generator efficiency is 0.95 according to the rated power conditions [37].

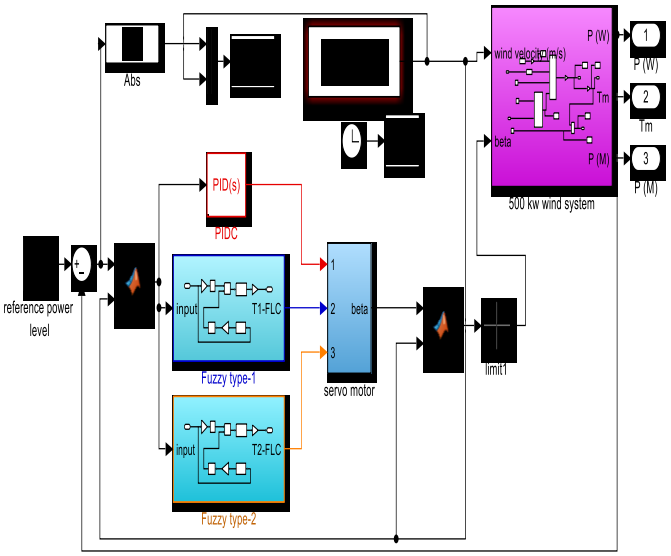

Fig. 9. Simulink model for WT with different controllers.

Table 1. Simulated WT system parameters [11]

rated output power	500 kilo Watt
cut in WS	3 m/s
rated WS	12 m/s
cut out WS	25 m/s
diameter of the rotor	48 m
turbine blade number	3
range of rotor speeds	10–30 rpm
generator type and number	PMSG - 2

6.1. Optimal PIDC

Figures. 10, 11, and 12 show the output power, pitch angle, and power error when the PIDC is used. The summation error of power signal (EPS) for the optimal PIDC based GA is 1.4212×10^{9} and based on PSO is 1.3812×10^{9}. PSO for tunning PIDC can reduced 2.81% in summation of EPS than the GA. Therefore, these results demonstrate that the PSO-based optimal PID provides better response than GA in terms of output power and errors between the reference and actual power generation in WT.

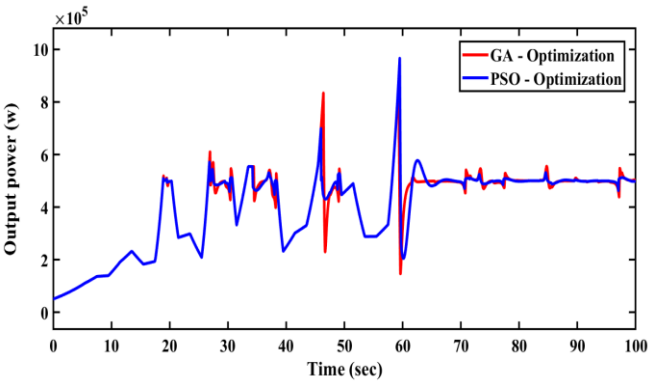

Fig. 10. Output power in PID-GA and PID-PSO.

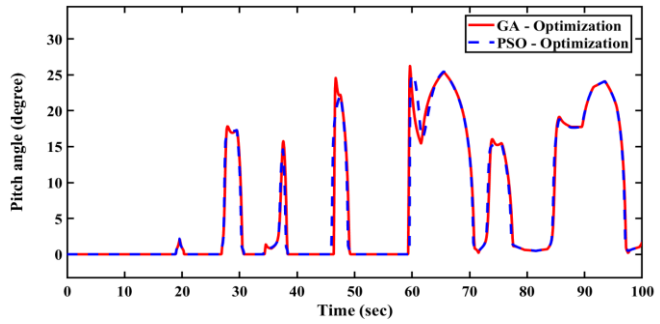

Fig. 11. Optimal BPA in PID-GA and PID-PSO.

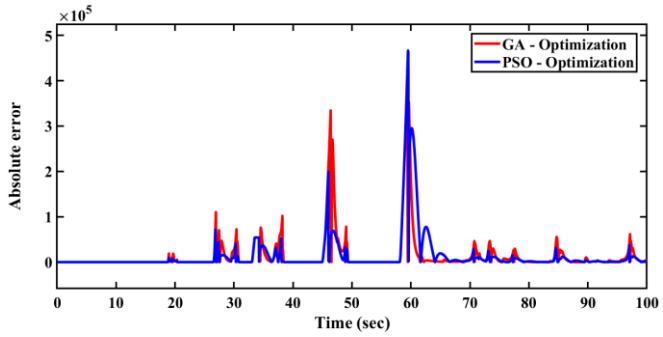

Fig. 12. Absolute error in PID-GA and PID-PSO.

6.2. T1-FLC

T1-FLC is tested based on two FIS: Mamdani and Sugeno. Figure. 13 displays FLC system inputs (error and derivative of error) as MF. Figure 14 shows the amount of change in pitch angle for only the Mamdani system. Table 2 contains a list of properties for Mamdani and Sugeno FIS that used in the design of T1-FLC. The Mamdani and Sugeno FIS are similar, however, Sugeno FIS does not involve clipping in output MF because it is either linear or constant. In this paper, Sugeno FIS is applied as a constant.

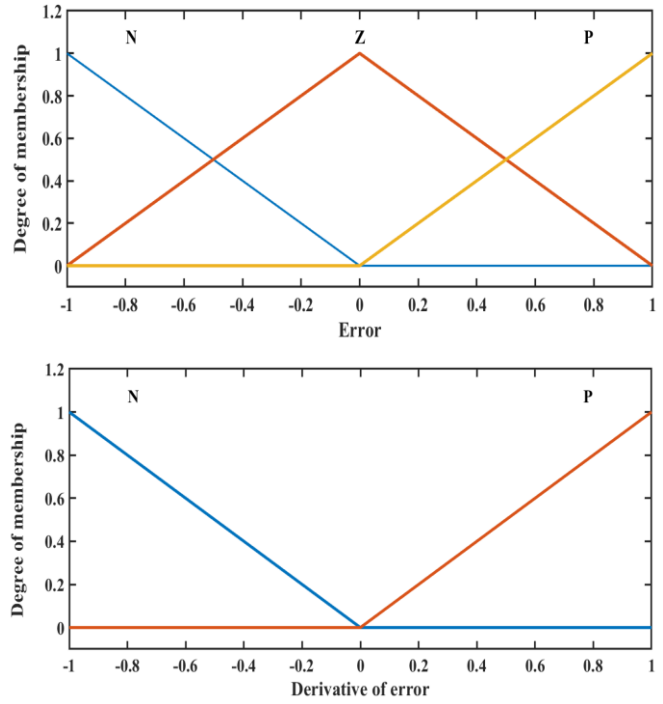

Fig. 13. The input variables fuzzy sets.

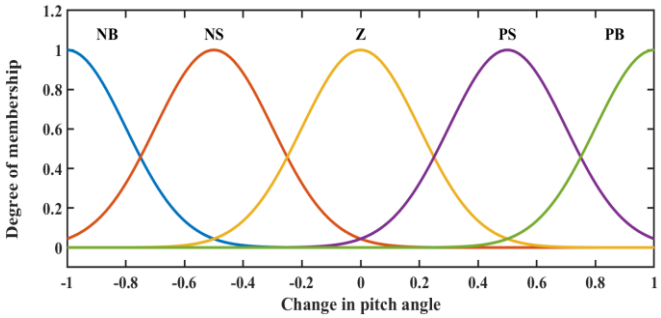

Fig. 14. The change in output variable fuzzy sets.

Table 2. properties for Mamdani and Sugeno FIS

Properties	**Mamdani**	**Sugeno**
And Method	Min	Min
Or Method	Max	Max
Implication Method	Min	Prod
Aggregation Method	Max	Sum
Defuzzification Method	Centroid	Weaver

As shown in Figure. 15, the fuzzy controller surface for Mamdani and Sugeno FIS illustrates the relationship between input and output variables as three-dimensional graphics. Also, two FIS rules are shown in Table 3.

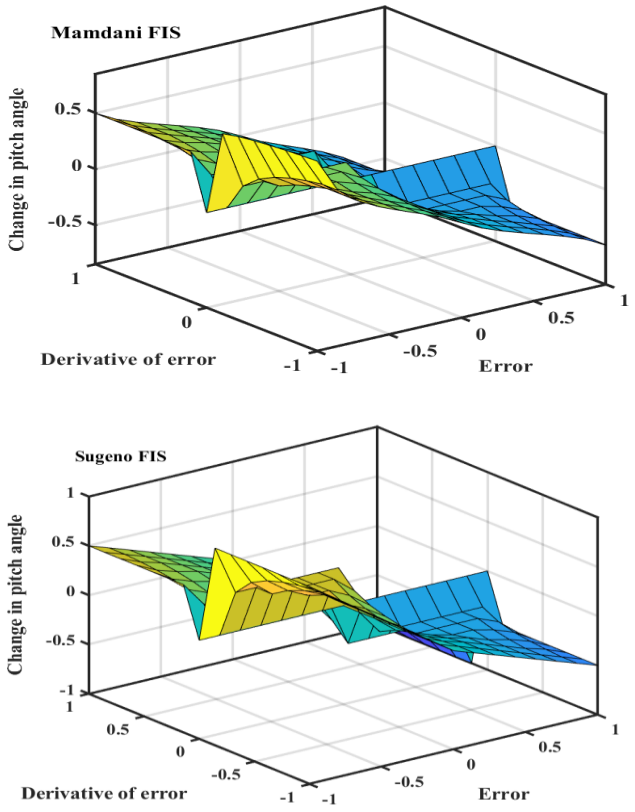

Fig. 15. FIS surface of T1-FLC for Mamdani and Sugeno.

Table 3. FIS Rules For Mamdani and Sugeno

Pitch angle chnage		Derivative of error	
		Negative	**Positive**
Error	**Negative**	PB	PS
	Zero	Z	Z
	Positive	NS	NB

Two input values in T1-FLC have three linguistic levels, one for error and two for the derivative of error as the following names: negative (N), zero (Z), and positive (P). While five linguistic levels in the output value as the following names: positive big (PB), positive small (PS), zero (Z), negative small (NS), and negative big (NB). The comparison in output power for two FIS (Mamdani and Sugeno) is shown in Figure. 16. As shown in this Figure, Sugeno FIS has better stability than Mamdani FIS. Figure. 17 show the comparison error signal between the Mamdani and Sugeno FIS. The summation EPS for T1-FLC based on Mamdani FIS is $1.3149\times10^{9}$and based on Sugeno is 9.9953×10^{8}. T1-FLC based on Sugeno FIS can reduced 23.98% in summation of EPS than T1-FLC based on Mamdani FIS. Furthermore, T1-FLC based on Sugeno FIS can reduced 27.63% in summation of EPS than the optimal tunning of PIDC by using PSO. Finally, two reasons make Sugeno better than Mamdani: first is Sugeno FIS using the weighted average of the rules to get crisp output and second is Sugeno possesses more flexibility in the system design and well suited to mathematical analysis.

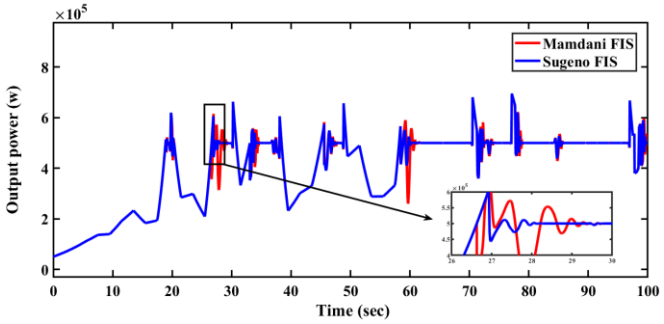

Fig. 16. Output power of T1-FLC for Mamdani and Sugeno.

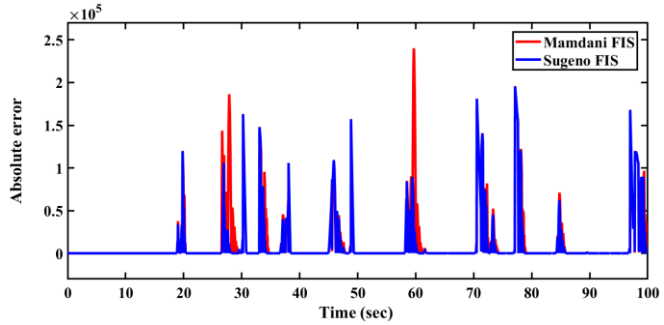

Fig. 17. Absolute error of T1-FLC for Mamdani and Sugeno.

6.3. T2-FLC

T2-FLC has been presented to address the limitations of T1-FLC when the level of uncertainty is overly high. As explain in previous section, the main differences between T1-FLC and T2-FLC are the footprint of uncertainty and type reduction used in T2-FLC. Figure. 18 shows the input of FLC (error and the derivative of error) as MF. These two inputs have three linguistic levels of error and two linguistic levels of the change in error under the following names: negative (N), zero (Z), and positive (P). The output has five linguistic levels under the following names: positive big (PB), positive small (PS), zero (Z), negative small (NS), and negative big (NB). Figure. 19 displays the output variable of T2-FLC for BPA controllers based on the Mamdani FIS.

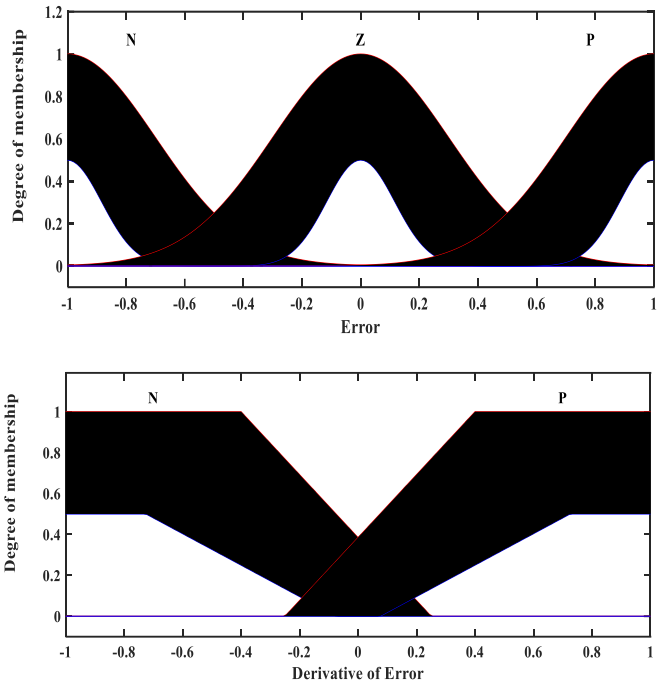

Fig. 18. The input variables fuzzy sets for T2-FLC.

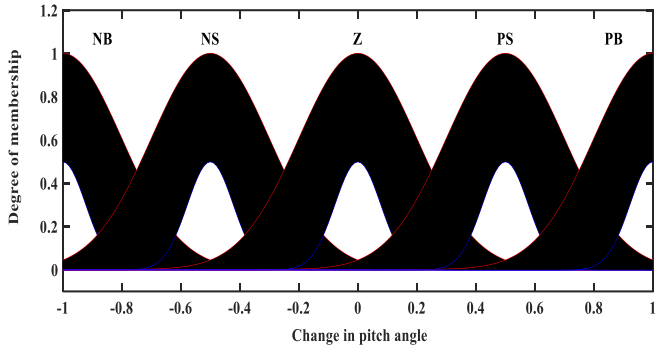

Fig. 19. The output variables fuzzy sets for T2-FLC.

The relationship between input and output variables is presented as three-dimensional graphics for the Mamdani and Sugeno FIS, as shown in Figures. 20 and 21. while the rules of the T2-FLC for the Mamdani and Sugeno FIS are the same as T1-FLC and as shown in Table 3.

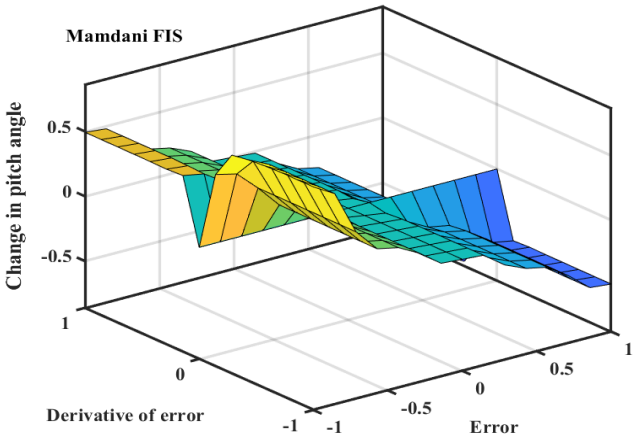

Fig. 20. FIS surface of T2-FLC for Mamdani.

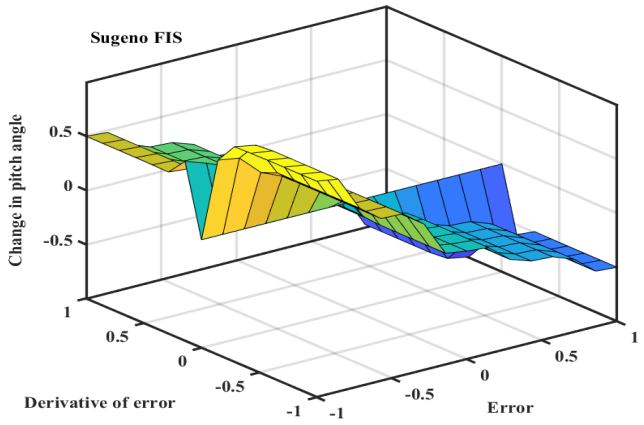

Fig. 21. FIS surface of T2-FLC for Sugeno.

The comparison in output power between two FIS (Mamdani and Sugeno) in T2-FLC is shown in Figure. 22, while the pitch angle is shown in Figure. 23.As shown in these Figures, Sugeno FIS has higher stable in output power than the Mamdani FIS.

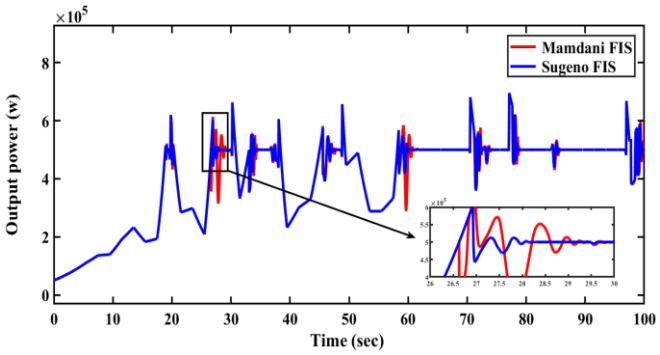

Fig. 22. Output power of T2-FLC for Mamdani and Sugeno.

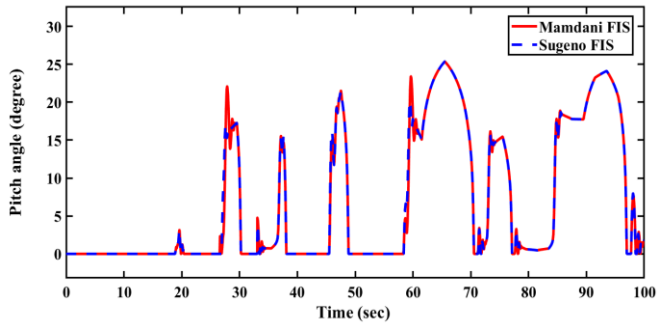

Fig. 23. BPA of T2-FLC for Mamdani and Sugeno.

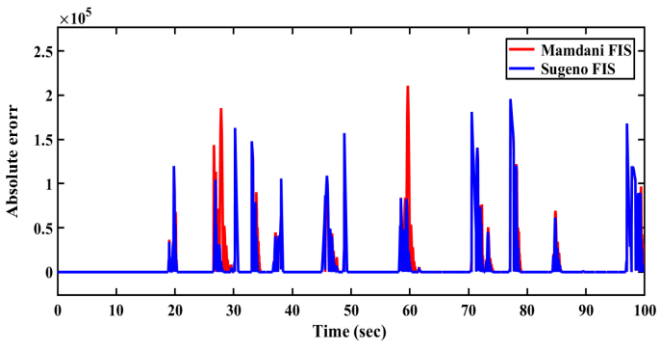

Fig. 24. Absolute error of T2-FLC for Mamdani and Sugeno.

Figure. 24 show the comparison in absolute power error signal between the Mamdani and Sugeno FIS. The summation EPS for T2-FLC based on Mamdani FIS is 1.2723×10^{9} and based on Sugeno is 9.9472×10^{8}. Therfore, T2-FLC based on Sugeno FIS can reduced 21.81% in summation of EPS than the Mamdani FIS. Also, T2-FLC based on Sugeno FIS has lower summation of EPS than Sugeno T1-FLC.

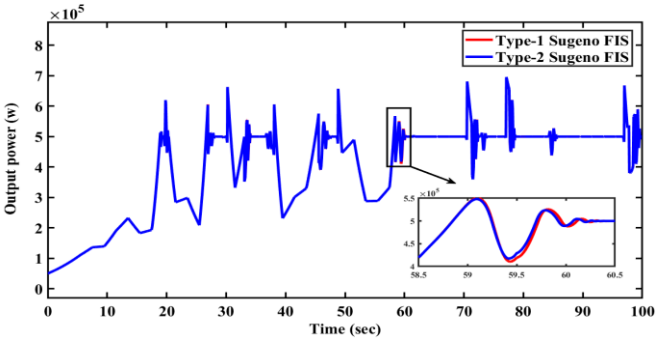

Fig. 25. Output power of T1-FLC and T2-FLC for Sugeno.

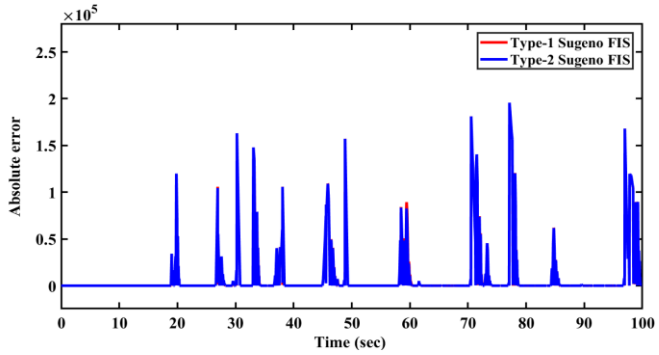

Fig. 26. Absolute error of T1-FLC and T2-FLC for Sugeno.

Figure. 25 shows a comparison in output power generation for only Sugeno FIS between T1-FLC and T2-FLC. Figure. 26 shows the difference in absolute error for the two controllers. As shown in both of Figs, the T2-FLC in Sugeno FIS has a better influence on power generation and lower error than the T1-FLC in Sugeno FIS. Since the Sugeno FIS for T2-FLC has greater flexibility and stability than Mamdani T2-FLC as well as Mamdani and Sugeno in T1-FLC, it has been applied to hybrid T2-FPIDC as explained in the next section.

6.4. Optimal Hybrid T2-FPIDC

Figure. 27 shows the fuzzification of input variables for the Sugeno FIS. The input membership values have five linguistic levels with the following names: negative high (NH), negative low (NL), zero (Z), positive low (PL), and positive high (PH). Furthermore, the five output linguistic levels with the following names: negative small (NS), negative medium (NM), negative medium-big (NMB), negative big (NB), and negative very-big (NVB). As shown in Table 4, The complete 75 control rules of the hybrid T2-FPIDC. Output power, BPA and absolute error when using GA and PSO optimization for the optimal tuning of PID controller applied in hybrid T2-FPIDC with Sugeno FIS are shown in Figure. 28, Figure. 29, and Figure 30 respectively. The summation EPS for optimal Sugeno HT2-FLC based on GA is 6.8481×10^{6} while based on PSO is 5.3460×10^{6}.

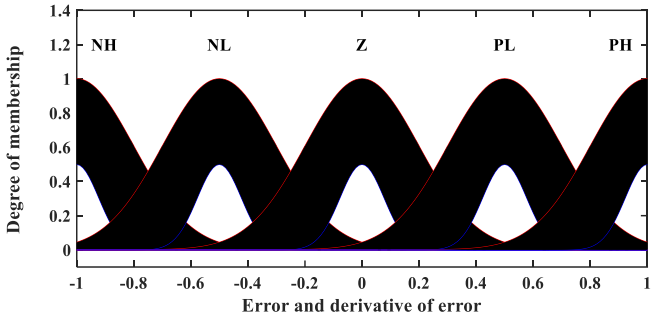

Fig. 27. The input variables fuzzy sets for hybrid T2-FPIDC.

Table 4. Rules of Dkp, Dki, Dkd for Sugeno FIS

Dkp		Derivative of error				
		NH	**NL**	**Z**	**PL**	**PH**
Error	**NH**	NS	NS	NS	NMB	NMB
	NL	NS	NM	NM	NB	NMB
	Z	NS	NM	NMB	NB	NB
	PL	NM	NM	NB	NB	NB
	PH	NMB	NMB	NB	NVB	NVB
Dki		Derivative of error				
		NH	**NL**	**Z**	**PL**	**PH**
Error	**NH**	NVB	NVB	NB	NB	NMB
	NL	NVB	NB	NB	NMB	NM
	Z	NVB	NMB	NMB	NB	NS
	PL	NM	NMB	NS	NB	NS
	PH	NS	NMB	NS	NVB	NS
Dkd		Derivative of error				
		NH	**NL**	**Z**	**PL**	**PH**
Error	**NH**	NS	NS	NM	NM	NMB
	NL	NS	NM	NM	NMB	NMB
	Z	NS	NM	NMB	NB	NVB
	PL	NM	NMB	NB	NB	NVB
	PH	NMB	NVB	NB	NVB	NVB

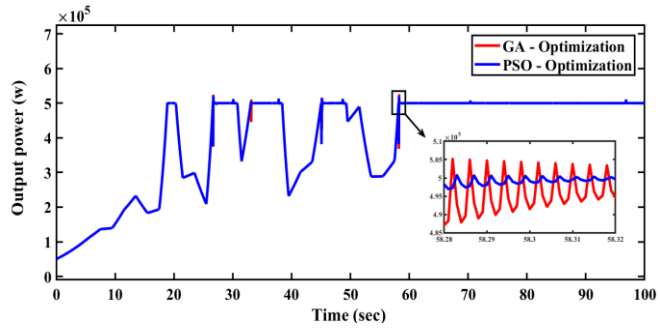

Fig. 28. Output power of hybrid T2-FPIDC for Sugeno FIS.

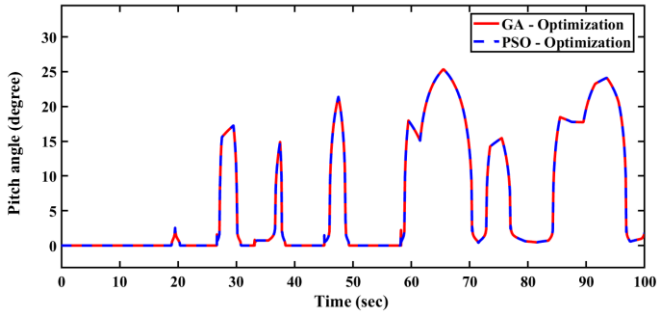

Fig. 29. Optimal BPA of hybrid T2-FPIDC for Sugeno FIS.

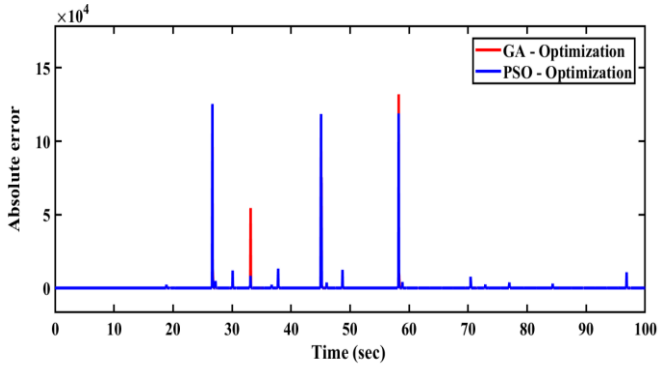

Fig. 30. Absolute error for hybrid T2-FPIDC with Sugeno.

As shown in Figure 28, Figure. 29 and Figure 30, Sugeno FIS in hybrid T2-FPIDC based on PSO has accurate results than the GA. Also, the comparison of summation error and maximum error for hybrid T2-FPIDC in different optimization algorithms. The hybrid T2-FPIDC based on the Sugeno FIS and PSO optimization for PID parameters tunning has 21.93% lower in Summation of EPS than the GA tunning of PID parameters. Furthermore, the optimal hybrid T2-FPIDC based on the Sugeno FIS and PSO can reduced 99.46% in the Summation of EPS than T2-FPIDC based on the Sugeno FIS. Therefore, the proposed optimal hybrid T2-FPIDC based on the Sugeno FIS and PSO can provide the best results in terms of stable output power generation with less error than the other controllers.

7. Conclusion

This paper proposes an accurate controller to find optimal BPA in HAWT. A 500-kw HAWT mathematical model was used to represent the output power generation under actual WS. Four different controllers: PIDC, T1-FLC, T2-FLC, and a hybrid T2-FPIDC were considered and compared to find the best controller for BPA controller in WT. Furthermore, Mamdani and Sugeno FIS were used to find the best FIS, as well as GA and PSO were compared in order to find the optimal tuning of PID based on reducing the summation of EPS. The simulation results showed that the PIDC based on PSO could reduce 2.81% in summation of EPS than the GA. Also, T1-FLC based on Sugeno FIS had 23.98% lower in summation of EPS than T1-FLC based on Mamdani FIS and 27.63% lower in summation of EPS than the optimal tunning of PIDC by using PSO. Sugeno FIS in T2-FLC provides 21.81% lower summation of EPS than Mamdani FIS in T2-FLC and lower summation of EPS than T1-FLC based on Sugeno FIS. On the other hand, hybrid T2-FPIDC based on Sugeno FIS and optimal PSO tunning of PID parameters had 21.93% lower in Summation of EPS than the GA tunning of PID parameters. Furthermore, the hybrid T2-FPIDC based on the Sugeno FIS and PSO provided more than 90% lower summation of EPS than Sugeno FIS in T2-FLC. Therefore, optimal hybrid T2-FPIDC based on PSO tuning with Sugeno FIS was the optimal and best controller in terms of stable power generation and reducing overall summation and maximum error signal.

References

[1] Daut, A. R. N. Razliana, Y. M. Irwan, and Z. Farhana, "A study on the wind as renewable energy in Perlis, Northern Malaysia", Energy Procedia, vol. 18, pp. 1428–1433, Jan. 2012.

[2] R. Al-Hajj, M. M. Fouad, A. Assi, and E. Mabrouk, "Short-term wind energy forecasting with independent daytime/nighttime machine learning models", 11th IEEE International Conference on Renewable Energy Research and Applications, ICRERA 2022, pp. 186–191, 2022.

[3] J. Fadil, Soedibyo, and M. Ashari, "Performance comparison of vertical axis and horizontal axis wind turbines to get optimum power output", 15th International Conference on Quality in Research (QiR): International Symposium on Electrical and Computer Engineering, Institute of Electrical and Electronics Engineers Inc., pp. 429–433, Dec. 2017.

[4] Tan and H. H. Wang, "A review on pitch angle control strategy of variable pitch wind turbines", Adv Mat Res, vol. 772, pp. 744–748, 2013.

[5] R. Hara, "Prediction of wind power generation output and network operation", Academic Press, 2016, ch.5.

[6] X. xing Yin, Y. gang Lin, W. Li, Y. jing Gu, X. jun Wang, and P. fei Lei, "Design, modeling and implementation of a novel pitch angle control system for wind turbine", Renew Energy, vol. 81, pp. 599–608, Sep. 2015.

[7] Jauch, S. M. Islam, P. Sørensen, and B. Bak Jensen, "Design of a wind turbine pitch angle controller for power system stabilisation", Renew Energy, vol. 32, no. 14, pp. 2334–2349, Nov. 2007.

[8] Bansal and K. Pandey, "Blade pitch angle and tip speed ratio control schemes for constant power generation of WECS", 1st IEEE International Conference on Power Electronics, Intelligent Control and Energy Systems, ICPEICES 2016, Institute of Electrical and Electronics Engineers Inc., Feb. 2017.

[9] Z. Jamal Mohammed, S. Enad Mohammed, and M. Obaid Mustafa, "Improving the performance of pitch angle control of variable speed wind energy conversion systems using fractional pi controller", 2022 Iraqi International Conference on Communication and Information Technologies (IICCIT), Institute of Electrical and Electronics Engineers (IEEE), pp. 209–215, Jan. 2023.

[10] X. S. Yang, S. Koziel, and L. Leifsson, "Computational optimization, modelling and simulation: recent trends and challenges", Procedia Computer Science, vol. 18, pp. 855–860, Jan. 2013.

[11] Z. Civelek, E. Çam, M. Lüy, and H. Mamur, "Proportional–integral–derivative parameter optimisation of blade pitch controller in wind turbines by a new intelligent genetic algorithm", IET Renewable Power Generation, vol. 10, no. 8, pp. 1220–1228, Sep. 2016.

[12] Khurshid, M.A. Mughal, A. Othman, T. Al-Hadhrami, H. Kumar, I. Khurshid, Arshad, J. Ahmad, "Optimal pitch angle controller for DFIG-based wind turbine system using computational optimization techniques", Electronics (Switzerland), vol. 11, no. 8, Apr. 2022.

[13] M. K. Al-Nussairi, S. D. Al-Majidi, A. R. Hussein, and R. Bayindir, "Design of a load frequency control based on a fuzzy logic for single area networks", 10th IEEE International Conference on Renewable Energy Research and Applications, ICRERA 2021, pp. 216–220, 2021.

[14] M. Ben Smida and A. Sakly, "Fuzzy pitch angle control for grid connected variable-speed wind turbine system", IREC 2016 - 7th International Renewable Energy Congress, Institute of Electrical and Electronics Engineers Inc., May 2016.

[15] Z. Civelek, E. Çam, M. Lüy, and G. Görel, "A new fuzzy controller for adjusting of pitch angle of wind turbine", The Online Journal of Science and Technology, vol. 6, no. 1, Jul. 2016, Accessed: Jun. 14, 2023.

[16] L. Saihi, Y. Bakou, A. Harrouz, M. Boura, I. Colak, and K. Kayisli, "Fuzzy-sliding mode control second order of wind turbine based on DFIG", 10th International Conference on Smart Grid, icSmartGrid 2022, pp. 296–300, 2022.

[17] A. Aziz, "Simulation model of wind turbine power control system with fuzzy regulation by mamdani and larsen algorithms", Al-Khwarizmi Engineering Journal, vol. 13, no. 2, Dec. 2017.

[18] K. A. Naik and C. P. Gupta, "Fuzzy logic based pitch angle controller/or SCIG based wind energy system", 2017 Recent Developments in Control, Automation and Power Engineering, RDCAPE 2017, Institute of Electrical and Electronics Engineers Inc., pp. 60–65, May 2018.

[19] Iqbal, D. Ying, A. Saleem, M. A. Hayat, and K. Mehmood, "Efficacious pitch angle control of variable-speed wind turbine using fuzzy based predictive controller", Energy Reports, Elsevier Ltd, pp. 423–427, Feb. 2020.

[20] I. A. H. I. C. Abdelhafid Benyounes, "A comparative modeling study of gas turbine using adaptive neural network, nonlinear autoregressive exogenous, and fuzzy logic approaches for modeling and control", International Journal of Smart grid, 2023.

[21] Z. Civelek, "Optimization of fuzzy logic (Takagi-Sugeno) blade pitch angle controller in wind turbines by genetic algorithm", Engineering Science and Technology, an International Journal, vol. 23, no. 1, pp. 1–9, Feb. 2020.

[22] K. A. Naik, C. P. Gupta, and E. Fernandez, "Advanced Type-2 fuzzy logic–based pitch-angle control strategy for wind energy system", Wind Engineering, vol. 44, no. 1, pp. 75–92, Feb. 2020.

[23] Bahraminejad, M. R. Iranpour, and E. Esfandiari, "Pitch control of wind turbines using IT2FL controller versus

T1FL controller", International Journal of Renewable Energy Research, vol. 4, no. 4, pp. 1065–1077, Dec. 2014.

[24] S. Nayak, S. S. Dash, and S. K. Kar, "Frequency regulation of hybrid distributed power systems integrated with renewable sources by optimized type-2 fuzzy PID controller", 9th International Conference on Smart Grid, icSmartGrid 2021, pp. 259–263, Jun. 2021.

[25] Villanueva, P. Ponce, and A. Molina, "Interval type 2 fuzzy logic controller for rotor voltage of a doubly-fed induction generator and pitch angle of wind turbine blades," IFAC-PapersOnLine, vol. 48, no. 3, pp. 2195–2202, Jan. 2015.

[26] Hamdan, M. M. M. Youssef, and O. Noureldeen, "Influence of interval type-2 fuzzy control approach for a grid-interconnected doubly-fed induction generator driven by wind energy turbines in variable-speed system", SN Appl Sci, vol. 5, no. 1, pp. 1–12, Jan. 2023.

[27] Z. Civelek, M. Lüy, E. Çam, and N. Barışçı, "Control of Pitch Angle of Wind Turbine by Fuzzy Pid Controller," Changed publisher: TSI Press, vol. 22, no. 3, pp. 463–471, Jul. 2015.

[28] Q. V. Ngo, C. Yi, and T. T. Nguyen, "The fuzzy-PID based-pitch angle controller for small-scale wind turbine", International Journal of Power Electronics and Drive Systems, vol. 11, no. 1, pp. 135–142, Mar. 2020.

[29] Serrano, J. E. Sierra-Garcia, and M. Santos, "Hybrid optimized fuzzy pitch controller of a floating wind turbine with fatigue analysis", Journal of Marine Science and Engineering, Vol. 10, Page 1769, vol. 10, no. 11, p. 1769, Nov. 2022.

[30] S. Pehlivan, B. Bahceci, and K. Erbatur, "Genetically optimized pitch angle controller of a wind turbine with fuzzy logic design approach", Energies, Vol. 15, Page 6705, vol. 15, no. 18, p. 6705, Sep. 2022.

[31] L. A. Zadeh, "The concept of a linguistic variable and its application to approximate reasoning—I", Information Sciences, vol. 8, no. 3, pp. 199–249, Jan. 1975.

[32] M. H. Fazel Zarandi, R. Gamasaee, and O. Castillo, "Type-1 to type-n fuzzy logic and systems", Studies in Fuzziness and Soft Computing, vol. 341, Springer Verlag, pp. 129–157, 2016.

[33] T. Kumbasar, "A simple design method for interval type-2 fuzzy pid controllers", Soft Computing, vol. 18, no. 7, pp. 1293–1304, Oct. 2014.

[34] M. K. Hussain and B. M. Alshadeedi, "Optimal design of high voltage composite insulators with grading rings in different configurations", Electric Power Systems Research, vol. 221, p. 109493, Aug. 2023.

[35] M. Rasham, M. K. Hussain, and M. H. Majeed, "Optimal characteristics of wind turbine to maximize capacity factor", AIP Conf Proc, vol. 2651, no. 1, Mar. 2023.

[36] M. A. Yurdusev, R. Ata, and N. S. Çetin, "Assessment of optimum tip speed ratio in wind turbines using artificial neural networks", Energy, vol. 31, no. 12, pp. 2153–2161, 2006.

[37] T. Corke and R. Nelson, Wind Energy Design, CRC Press, 2018, pp.143-168.